doi:10.1016/j.jmb.2009.06.050 J. Mol. Biol. (2009) 392, 48–62

JMB

Available online at www.sciencedirect.com

ScienceDirect

ELSEVIER

Effects of Chloride Ion Binding on the Photochemical Properties of *Salinibacter* Sensory Rhodopsin I

Daisuke Suzuki[1], Yuji Furutani[2], Keiichi Inoue[3], Takashi Kikukawa[4], Makoto Sakai[3], Masaaki Fujii[3], Hideki Kandori[2], Michio Homma[1] and Yuki Sudo[1,5]*

[1]*Division of Biological Science, Graduate School of Science, Nagoya University, Chikusa-ku, Nagoya 464-8602, Japan*

[2]*Department of Frontier Materials, Nagoya Institute of Technology, Showa-ku, Nagoya 466-8555, Japan*

[3]*Chemical Resources Laboratory, Tokyo Institute of Technology, 4259 Nagatsuta-cho, Midori-ku, Yokohama 226-8503, Japan*

[4]*Division of Biological Sciences, Graduate School of Science, Hokkaido University, Sapporo 060-0810, Japan*

[5]*PRESTO, Japan Science and Technology Agency (JST), 4-1-8 Honcho Kawaguchi, Saitama 332-0012, Japan*

Received 26 January 2009; received in revised form 31 May 2009; accepted 18 June 2009
Available online 26 June 2009

Edited by W. Baumeister

Microbial organisms utilize light not only as energy sources but also as signals by which rhodopsins (containing retinal as a chromophore) work as photoreceptors. Sensory rhodopsin I (SRI) is a dual photoreceptor that regulates both negative and positive phototaxis in microbial organisms, such as the archaeon *Halobacterium salinarum* and the eubacterium *Salinibacter ruber*. These organisms live in highly halophilic environments, suggesting the possibility of the effects of salts on the function of SRI. However, such effects remain unclear because SRI proteins from *H. salinarum* (*Hs*SRI) are unstable in dilute salt solutions. Recently, we characterized a new SRI protein (*Sr*SRI) that is stable even in the absence of salts, thus allowing us to investigate the effects of salts on the photochemical properties of SRI. In this study, we report that the absorption maximum of *Sr*SRI is shifted from 542 to 556 nm in a Cl^--dependent manner with a K_m of 307±56 mM, showing that Cl^--binding sites exist in SRI. The bathochromic shift was caused not only by NaCl but also by other salts (NaI, NaBr, and $NaNO_3$), implying that I^-, Br^-, and NO_3^- can also bind to *Sr*SRI. In addition, the photochemical properties during the photocycle are also affected by chloride ion binding. Mutagenesis studies strongly suggested that a conserved residue, His131, is involved in the Cl^--binding site. In light of these results, we discuss the effects of the Cl^- binding to SRI and the roles of Cl^- binding in its function.

Keywords: sensory rhodopsin; color tuning; anion binding; signal transduction; phototaxis

Introduction

Animals, plants, archaea, and bacteria utilize light not only as energy sources but also as signals.[1–3] Microorganisms respond and adapt to photostimulation, in which light energy is absorbed by rhodopsins, which are seven-transmembrane helix proteins containing retinal as a chromophore.[4–7] The archaeon *Halobacterium salinarum* has two ion-pumping rhodopsins, bacteriorhodopsin (BR) and halorhodopsin (HR), which work as a light-driven proton pump and a chloride ion pump to produce energy, respectively[4,5] (Fig. 1). The molecular properties of BR have been extensively studied not only as a model of photoactive proteins but also as a model of membrane proteins.[8] In addition, archaea have two other microbial rhodopsins, sensory rhodopsin I (SRI) and sensory rhodopsin II (SRII, also

*Corresponding author. E-mail address: 4sudo@bunshi4.bio.nagoya-u.ac.jp.

Abbreviations used: BR, bacteriorhodopsin; DDM, *n*-dodecyl-β-D-maltoside; HR, halorhodopsin; PG, L-α-phosphatidylglycerol; PSB, protonated Schiff base; SRI, sensory rhodopsin I; SRII, sensory rhodopsin II.

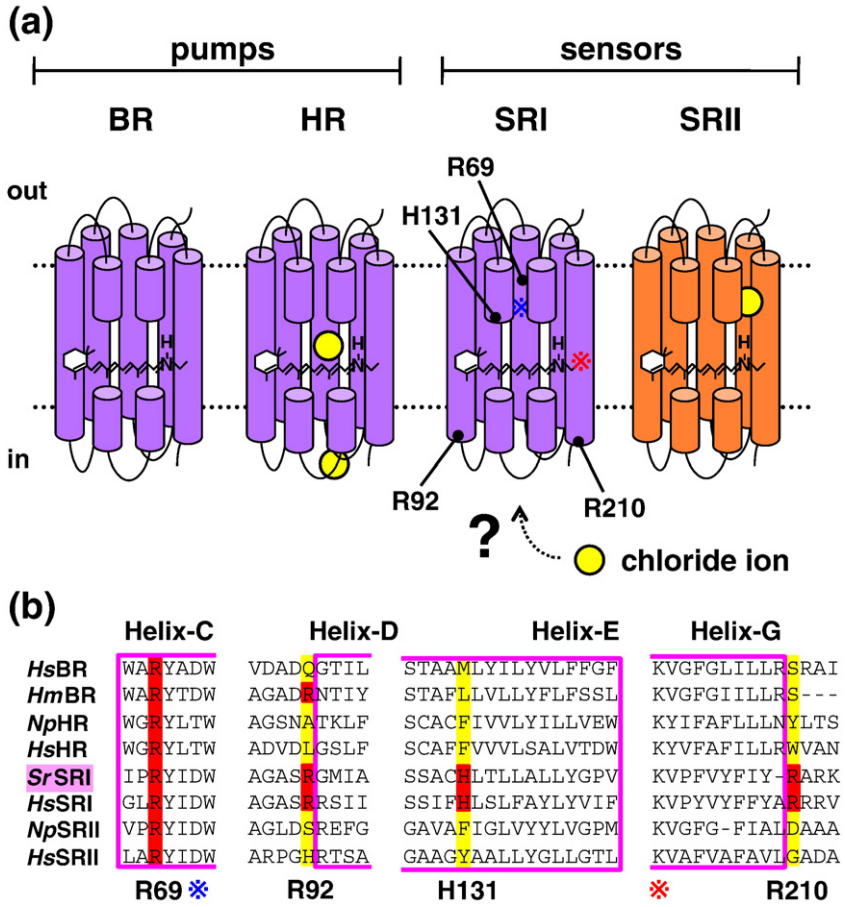

Fig. 1. (a) Chloride-binding models of microbial rhodopsins. Rhodopsins have seven-transmembrane helices and are covalently bound to an all-trans retinal chromophore at a conserved lysine residue in the G-helix via a PSB bond. BR, HR, and SRII have 0, 2, and 1 chloride-binding site(s) inside the protein moiety at neutral pH, respectively. The chloride ion interacts with the PSB and Arg200/Thr203 in *H. salinarum* HR (*Hs*HR) [Lys215/Thr218 in *N. pharaonis* HR (*Np*HR)]. For a repellent photosensor, *N. pharaonis* SRII (*Np*SRII), the chloride ion binds to a residue near Arg72 located at the extracellular side of the transmembrane region. For an attractant and repellent photosensor, SRI, the binding of chloride ion to the protein is unclear because of the protein instability of *Hs*SRI in low salt conditions. (b) Alignment of putative amino acid sequences of microbial rhodopsins. Names of microbial rhodopsins and sources from top are as follows: *Hs*BR, BR from *H. salinarum* (GenBank™ code: 5953595); *Hm*BR, BR from *Haloarcula marismortui* (3128463); *Np*HR, HR from *N. pharaonis* (3702828); *Hs*HR, HR from *H. salinarum* (5952411); *Sr*SRI, SRI from *S. ruber* (3852586); *Hs*SRI, SRI from *H. salinarum* (5953902); *Np*SRII, SRII from *N. pharaonis* (3703211); *Hs*SRII, SRII from *H. salinarum* (5953098). Blue and red asterisks indicate counter ion (except for HR) and conserved Lys residue that bind to retinal, respectively. Arg69, Arg92, His131, and Arg210 indicate candidates of the positively charged residue whose ionic state may give rise to binding between Cl^- and *Sr*SRI.

known as phoborhodopsin, pR) (Fig. 1).[6,7] SRI and SRII work as sensors to transfer signals to the cytoplasm and form 2:2 complexes with their cognate transducer proteins, halobacterial transducer protein for SRI (HtrI) and halobacterial transducer protein for SRII (HtrII), respectively.[9,10] SRII functions as a photosensory receptor for negative phototaxis to blue light (500 nm).[7,11]

SRI can be activated by orange light (560–580 nm) and shows an ability to mediate opposing signals depending on the light color by photochromic, one- and two-photon reactions.[12,13] Light absorption triggers *trans–cis* photoisomerization of retinal chromophores, leading to cyclic chemical reactions (the photocycle) consisting of some sequential intermediate states (K and M).[8] During the photocycle, light signals are transmitted from the SRI/HtrI complex to the two-component signal transduction cascade consisting of kinases (CheA and CheY),[13] which regulates the rotation direction of the flagellar motor, resulting in positive phototaxis.[12,14] The absorption spectrum of SRI (λ_{max} = 587 nm) overlaps the spectra of BR (λ_{max} = 570 nm) and HR (λ_{max} = 580 nm).[7,8] Thus, SRI functions as an attractant sensor for energy production by these ion-pumping rhodopsins.[12] SRI can also function as a repellent sensor.[12] It absorbs orange light and forms a long-lived M photointermediate, which then forms the P510 intermediate upon a second photon absorption by near-UV light.[12,13] Only when the photocycle signals are produced through the P510

intermediate does SRI induce a negative phototaxis to avoid harmful near-UV light.[12] The X-ray crystal structures of BR, HR, SRII, and the SRII/HtrII complex have been solved over the past 10 years;[10,15–18] however, almost no structural information at the atomic level has been gained for SRI because of the instability of SRI from *H. salinarum* (*Hs*SRI). Thus, the molecular mechanism of the phototaxis function of SRI is still unclear.

Halobacteria and *Salinibacter ruber* live in highly halophilic environments,[19] suggesting the possibility of the effect(s) of salts on the functions of retinal proteins. BR does not bind any chloride ion under physiological conditions, whereas HR binds a chloride ion (or chloride ions) inside the protein (Fig. 1).[16,20] This is quite reasonable since HR works as a light-driven chloride ion pump. The crystal structure of HR revealed that the chloride ion is hydrated by a cluster of three water molecules that form hydrogen bonds with neighboring amino acids including Arg108, Thr111, and Lys242 in *H. salinarum* HR (*Hs*HR) (Arg123, Thr126, and Lys256 in *Natronomonas pharaonis* HR, *Np*HR).[16] The anion itself interacts with the proton of the protonated Schiff base (PSB) and the hydroxyl group of Ser115 in *Hs*HR (Ser130 in *Np*HR). It has been assumed that another anion binding site is required for the release of the chloride ion from the extracellular side to the cytoplasmic side.[21] The candidate residues have been suggested to be Arg200 and Thr203 in *Hs*HR (Lys215 and Thr218 in *Np*HR).[21] The question remains about sensory rhodopsins. *Np*SRII exhibits fast proton release in the presence of chloride ions.[22] It releases a proton before the M decay, followed by slower proton uptake. However, in the absence of chloride ions, *Np*SRII does not exhibit fast proton release.[22] Furthermore, the chloride ion plays an important role in maintaining the conformation and in regulating the pK_a of the PSB in the D193N mutant of SRII.[23] One of the X-ray crystallographic structures of *Np*SRII clearly demonstrates that a putative chloride ion binding site exists near Arg72 (Fig. 1).[18] Recently, Kitade *et al.* reported the Cl^--induced difference attenuated total reflection Fourier transform infrared spectroscopy in the aqueous phase. In this article, they concluded that binding of Cl^- to SRII accompanies protonation of a carboxylic acid (C=O stretch at 1724 cm^{-1}), and the amino acid was identified as Asp193, because the corresponding band is shifted to 1705 cm^{-1} in the D193E mutant protein.[24]

It remains unknown whether SRI binds to a chloride ion (or to chloride ions). The binding effect is still unclear because *Hs*SRI is unstable in dilute salt solutions. We recently cloned and characterized a novel SRI protein from a eubacterium *S. ruber* (*Sr*SRI), which is the first eubacterial SRI identified as a functional protein.[25] *Sr*SRI maintains its structure and functions even in dilute salt conditions whereas *Hs*SRI denatured within 1 h under those conditions.[25] Thus, *Sr*SRI can be a key protein to investigate the functions of SRI at the molecular level. In fact, we have already demonstrated the unique structure and structural changes of *Sr*SRI upon the formation of the K and the M intermediates by Fourier transform infrared spectroscopy.[26] The high stability of *Sr*SRI enabled us to obtain accurate spectra using UV–Vis spectroscopy, high-performance liquid chromatography (HPLC) analysis, and time-resolved laser spectroscopy. In this study, we report the effects of chloride ion binding on the photochemical properties of *Sr*SRI.

Results

Spectral red shift of *Sr*SRI in the presence of NaCl

UV–Vis absorption spectra of purified *n*-dodecyl-β-D-maltoside (DDM)-solubilized *Sr*SRI over the spectral range from 420 to 720 nm were obtained as shown in Fig. 2a. The λ_{max} of *Sr*SRI in the absence of NaCl, where the ionic strength was kept constant with 333 mM Na_2SO_4, was located at 542 nm, while the λ_{max} of *Sr*SRI with 1 M NaCl was located at 556 nm, showing a 14-nm spectral red shift ($\Delta\upsilon = -130\ cm^{-1}$) with a similar molar extinction coefficient (Fig. 2a). The red shift was also observed in L-α-phosphatidylglycerol (PG)-reconstituted *Sr*SRI in which the absorbance maxima were at 558 and 544 nm with 1 M NaCl and without NaCl (333 mM Na_2SO_4), respectively, implying that the red shift was not affected by the different conditions (detergent *versus* lipid) (data not shown).

To investigate whether the spectral change was caused by the difference of retinal configuration, we used HPLC analysis, since it is well known that a decrease in *13-cis* retinal isomer causes a spectral red shift in microbial rhodopsins.[27] Figure 2b shows the retinal isomer composition. *Sr*SRI without NaCl (333 mM Na_2SO_4) contains more than 95.1% all-trans retinal with a small proportion of *13-cis* retinal as well as *Sr*SRI with 1 M NaCl (95.7%),[25] indicating that the spectral red shift is not caused by a change in retinal configuration. Similar results were obtained when the PG-reconstituted *Sr*SRI was used (data not shown). In retinal proteins (except for HR), the PSB is stabilized by a deprotonated aspartate as a counterion (Asp72 for *Sr*SRI). A spectroscopic pH titration was performed to estimate the pK_a value of Asp72 because the spectral red shift is caused by protonation of the counterion. Difference spectra from pH 8.5 to pH 6.75, 4.68, and 4.15 were shown over a spectral range from 460 to 750 nm (Fig. 2c). The spectra were obtained in the pH range from 8.5 to 3.5 because a denatured form occurred at low pH (<3.5). The experiments were carried out in a chloride-free buffer containing 333 mM Na_2SO_4 to circumvent chloride interactions with the proteins. The titration curves were fitted well using the Henderson–Hasselbach equation (Fig. 2d),[28] and the pK_a value of Asp72 for PG-reconstituted *Sr*SRI was estimated as 4.2 in the chloride-free buffer compared with the previously reported pK_a value of 4.3 in 1 M NaCl (dotted lines in Fig. 2d).[25] Thus, the

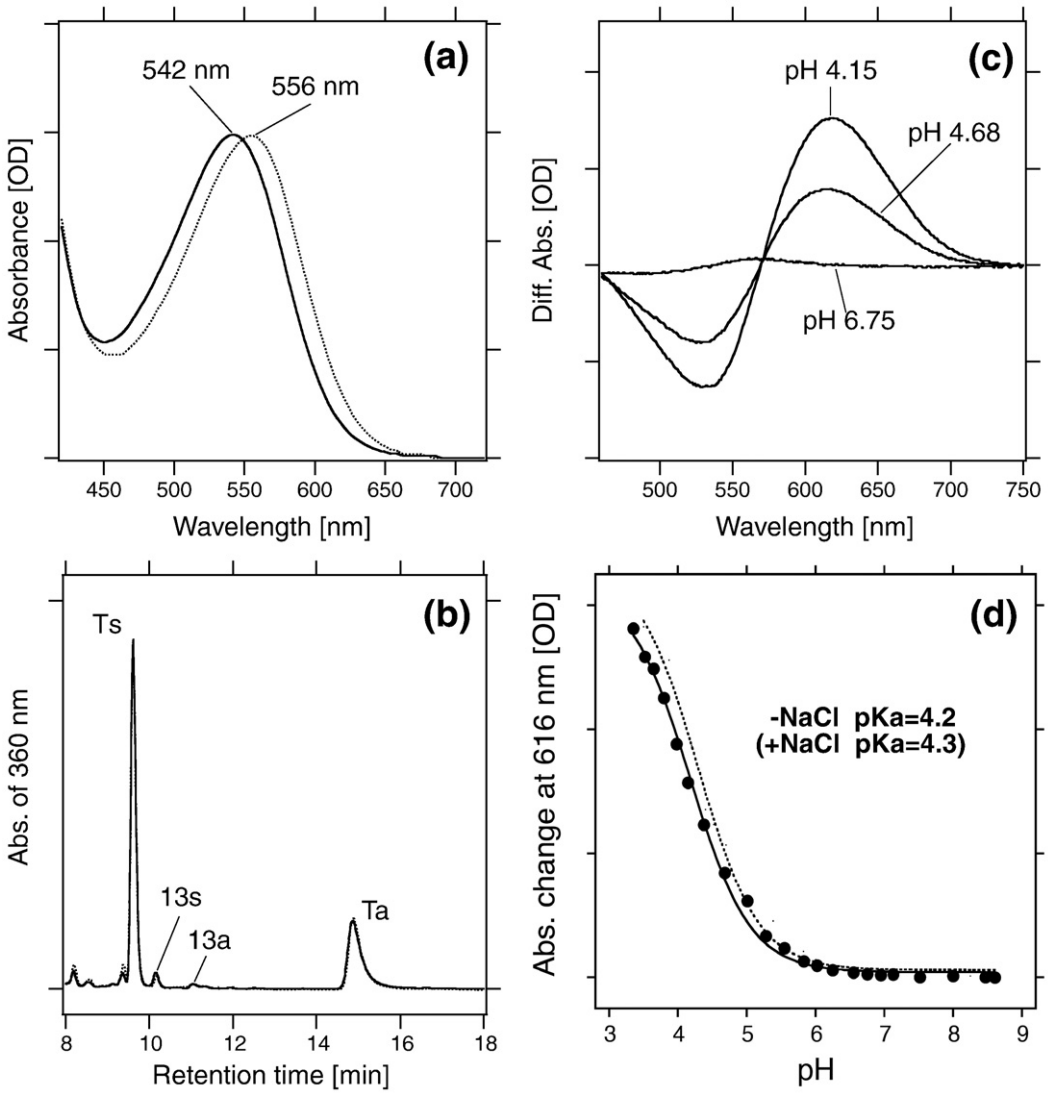

Fig. 2. (a) Absorption spectra of DDM-solubilized *Sr*SRI with 1 M NaCl (dotted line) and without NaCl (continuous line) over a spectral range from 420 to 720 nm. The ionic strength was kept constant using 333 mM Na_2SO_4. The samples were suspended in 50 mM Tris–H_2SO_4, pH 7.0, and 0.1% DDM. (b) Chromophore configuration extracted from DDM-solubilized *Sr*SRI in 1 M NaCl (dotted line) or 333 mM Na_2SO_4 (continuous line). The detection beam was set at 360 nm. Ts, Ta, 13s, and 13a indicate peaks of all-trans 15-syn, all-trans 15-anti, 13-cis 15-syn, and 13-cis 15-anti, respectively. The molar composition of retinal isomers was calculated from the peak areas in the HPLC patterns. The spectrum for 0 M NaCl (continuous line) is normalized by multiplying a factor of 0.84 for the sake of comparison. (c) Difference absorption spectra of PG-reconstituted *Sr*SRI at pH 4.15, 4.68, and 6.75 over a spectral range from 460 to 750 nm. Each sample was suspended in six mix buffers (citric acid, Mes, Hepes, Mops, Ches, or Caps, 10 mM each) with 333 mM Na_2SO_4. The pH was adjusted to the desired value by the addition of concentrated H_2SO_4. Each spectrum was obtained by subtracting that obtained at pH 8.5. (d) pH titration curves of the counterion (Asp72) in *Sr*SRI in the presence (dotted line) or absence of NaCl (filled circles). Titration curves were analyzed using the Henderson–Hasselbach equation with a single pK_a value. The temperature was kept at 20 °C. Data for *Sr*SRI with 1 M NaCl were reproduced from a previous study for comparison. One division of the *y*-axis of (a), (c), and (d) corresponds to 0.1, 0.2, and 0.2 absorbance units, respectively.

chloride-dependent spectral red shift is not derived from the change of pK_a of Asp72.

Anion binding to *Sr*SRI and its K_m value

To estimate the binding parameter K_m, we measured the absorption spectra of *Sr*SRI under various NaCl concentrations (0–4 M) (Fig. 3). Figure 3a shows the visible spectral changes obtained by titration with NaCl over a spectral range from 420 to 700 nm. The NaCl concentrations of each spectrum were 0, 10, 100, 200, 500, 1000, and 4000 mM. The results clearly show that the λ_{max} of *Sr*SRI was shifted from 542 to 556 nm by the addition of NaCl to the desalted buffer. The different spectra show the increase in absorbance at 586 nm and have an isosbestic point at about 550 nm (Fig. 3b), indicating an equilibrium between the chloride-ion-bound and -unbound forms of *Sr*SRI. The absorbance changes at 586 nm were plotted against the NaCl concen-

trations (Fig. 3c, filled circles), and the K_m values were calculated using the Michaelis–Menten equation and were estimated as 307±57 mM for the DDM-solubilized *Sr*SRI (filled circles) and 600±147 mM for the PG-reconstituted *Sr*SRI (open circles).

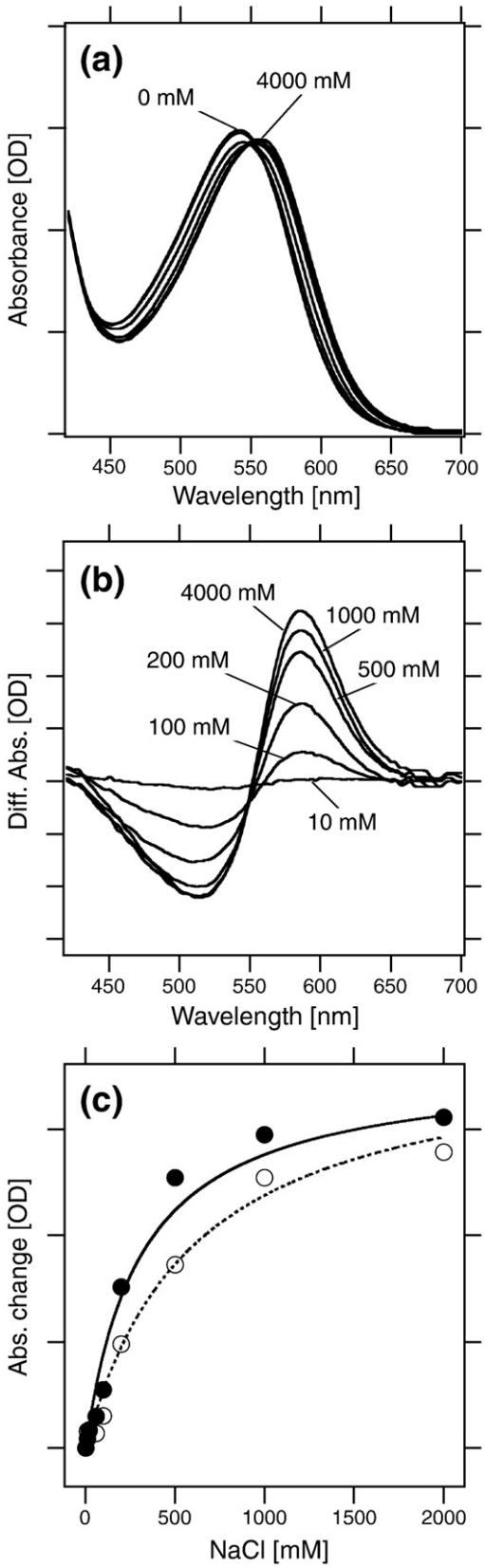

In chloride ion-pumping rhodopsin HR, various anions (such as iodine, bromine, and nitrate ions) can also interact with the protein moiety. The ~25-nm spectral blue shift was observed in an anion-dependent manner, and HR can pump the anions by illumination.[20] The absorption spectra of *Sr*SRI in the presence of various salts were obtained by adding the following salts to the desalted buffer: Fig. 4a–e for NaI, $NaNO_3$, NaBr, Na_2SO_4, and NaF, respectively. The spectral red shift occurred in an anion-dependent manner (for iodine, bromine and nitrate ions) as was observed with the chloride ion (Fig. 4). The absorbance changes were plotted against the anion concentrations, and the K_m values of each anion were estimated as 63±11 mM for the iodine ion, 63±10 mM for the nitrate ion, and 121±16 mM for the bromine ion (Fig. 4f). In contrast, Na_2SO_4 and NaF did not cause a spectral shift, suggesting that SO_4^{2-} and F^- are too large or too small to bind to *Sr*SRI, respectively. Interestingly, the order of the K_m values for the various anions is the same as the Hofmeister series ($SO_4^{2-} > F^- > Cl^- > Br^- > NO_3^- > I^-$),[29] which represents their order of hydrophobicity and their tendency to stabilize the structured low-density water.

Effects of chloride ion binding to *Sr*SRI on its photocycle

*Sr*SRI absorbs orange light and triggers a cyclic reaction that is composed of a series of intermediates, designated alphabetically (K and M intermediates).[25] An important question is whether the photocycle is affected by the chloride ion binding to the protein moiety. The trans–cis photoisomerization of the retinal chromophore leads to the formation of the red-shifted K intermediate.[26] We analyzed the effects of chloride ion binding to *Sr*SRI on the decay rate constant of the K intermediate and its molar extinction coefficient. The light minus dark difference absorption spectra were obtained over a time range from 300 ns to 1000 μs (Fig. 5). The spectral red shifts indicate the formation of the K intermediate of *Sr*SRI both in the presence and in the absence of NaCl, while the molar extinction coefficient decreased in the condition without NaCl (333 mM Na_2SO_4). Figure 5b and d show the time courses of

Fig. 3. (a) Absorption spectrum changes of DDM-solubilized *Sr*SRI by adding NaCl to the desalted buffer (50 mM Tris–H_2SO_4, pH 7.0, and 0.1% DDM) over a spectral range from 420 to 700 nm. NaCl concentrations are 0, 10, 100, 200, 500, 1000, and 4000 mM. (b) Difference absorption spectra by adding NaCl to the desalted *Sr*SRI sample in the spectral range. Each spectrum corresponds to 10, 100, 200, 500, 1000, or 4000 mM NaCl. (c) Absorbance changes at 586 nm were plotted against NaCl concentrations, and K_m values were calculated using the Michaelis–Menten equation and were estimated as 307±57 mM in the DDM-solubilized *Sr*SRI (filled circles) and 600±147 mM in the PG-reconstituted *Sr*SRI (open circles). One division of the *y*-axis of (a), (b), and (c) corresponds to 0.1, 0.02, and 0.02 absorbance units, respectively.

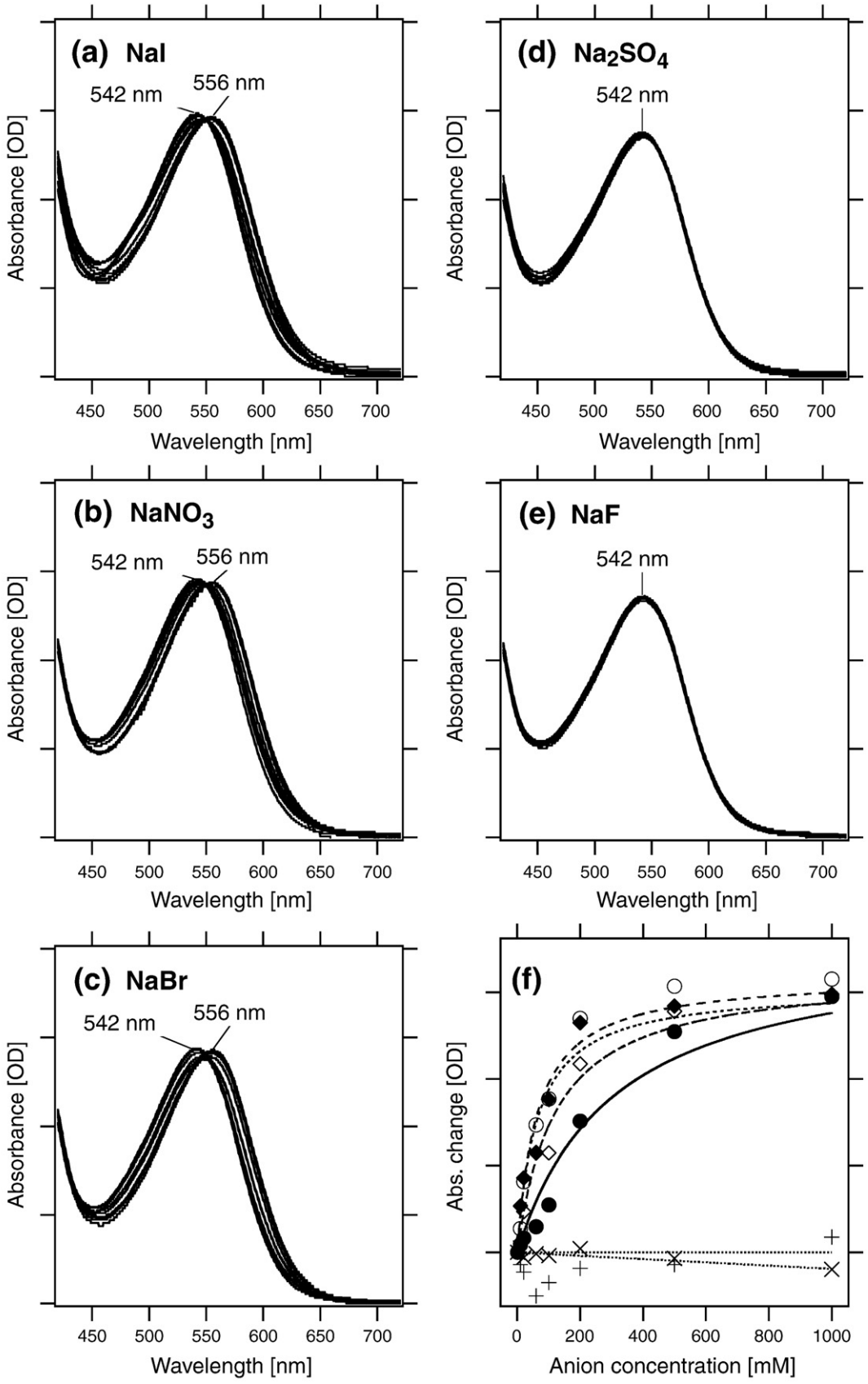

Fig. 4 (*legend on next page*)

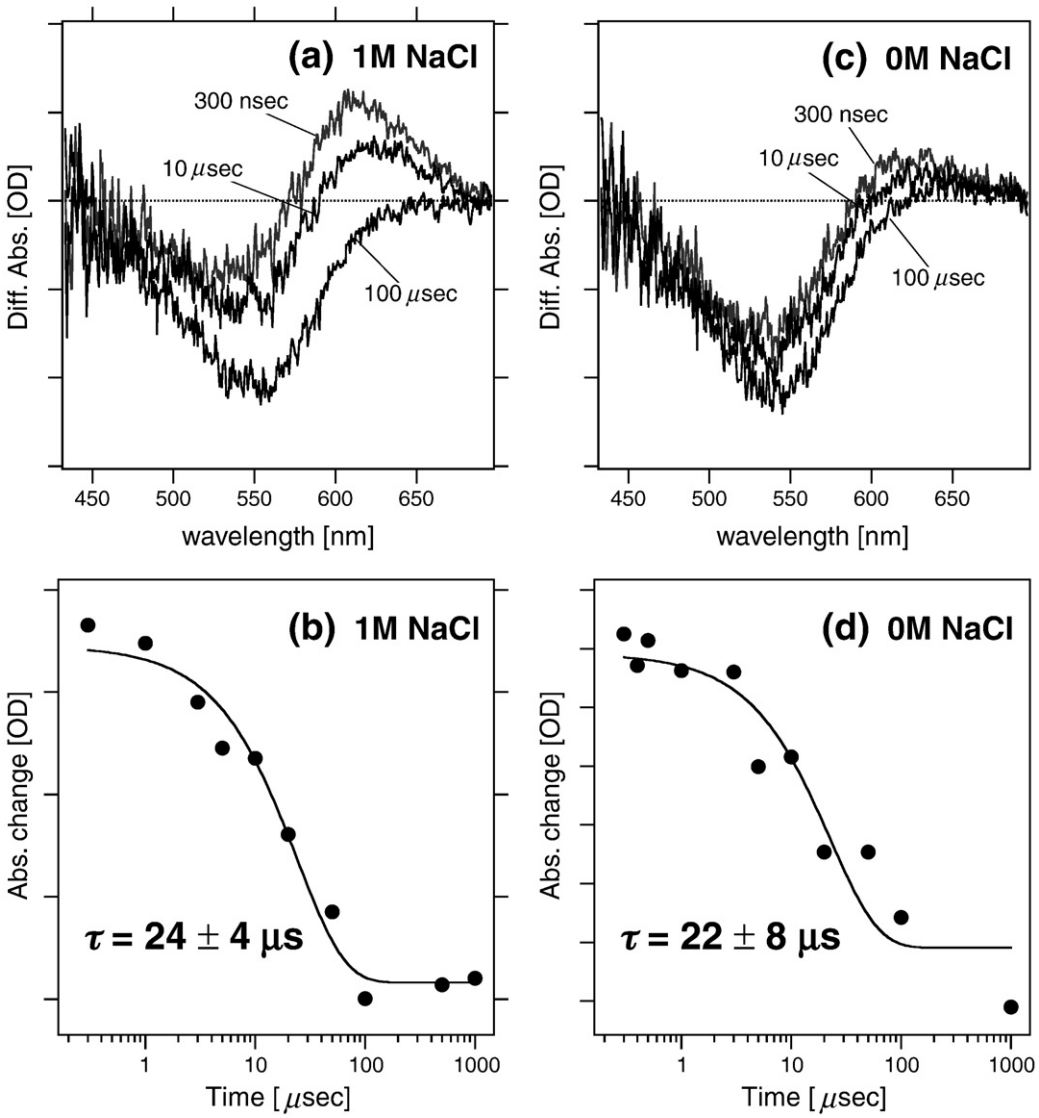

Fig. 5. Flash-induced difference absorption spectra of *Sr*SRI with 1 M NaCl (a) or without NaCl (333 mM Na_2SO_4) (c) over a spectral range from 430 to 700 nm and a time range from 300 ns to 1000 μs. Curves in (a) and (c) are spectra of 300 ns, 10 μs, and 100 μs after the illumination. Flash-induced kinetic data of *Sr*SRI with 1 M NaCl (b) or without NaCl (333 mM Na_2SO_4) (d) at 600 nm representing the K decay. The data fit well with a single exponential decay equation, and the half-time was estimated as 24±4 μs for *Sr*SRI with 1 M NaCl and 22±8 μs for *Sr*SRI without NaCl (333 mM Na_2SO_4). The temperature was kept at 25 °C. One division of the *y*-axis of (a)–(d) corresponds to 0.05, 0.02, 0.05, and 0.005 absorbance units, respectively.

the absorbance changes at 600 nm in solutions containing 1 M NaCl or without NaCl (333 mM Na_2SO_4), respectively. It was seen that 1 M NaCl was enough for *Sr*SRI to bind the chloride ion because the K_m value was about 300 mM (Fig. 3). In fact, the curves fit well by a single exponential decay equation, and the half-times were estimated as 24± 4 μs for *Sr*SRI with 1 M NaCl and 22±8 μs for *Sr*SRI without NaCl (333 mM Na_2SO_4), indicating that the decay rate of K intermediate of *Sr*SRI is not altered by chloride ion binding.

Besides the K intermediate, a long-lived M intermediate has been identified in *Sr*SRI,[25] which is believed to be a signaling intermediate for the

Fig. 4. Effect of various anions on the absorption spectrum of DDM-solubilized *Sr*SRI for (a) NaI, (b) $NaNO_3$, (c) NaBr, (d) Na_2SO_4, and (e) NaF. The spectra of *Sr*SRI by adding various salts to the desalted buffer (50 mM Tris–H_2SO_4, pH 7.0, and 0.1% DDM) are shown over a spectral range from 420 to 720 nm. (f) Anion binding to DDM-solubilized *Sr*SRI detected by measuring absorbance change at 586 nm. The curves for various anions are the best-fitted curves of each plot to the Michaelis–Menten equation. Filled circles, data set of Cl^-; open circles, I^-; filled diamonds, NO_3^-; open diamonds, Br^-; X marks, F^-; cross shapes, SO_4^{2-}. One division of the *y*-axis of (a)–(e) and (f) corresponds to 0.1 and 0.02 absorbance units, respectively.

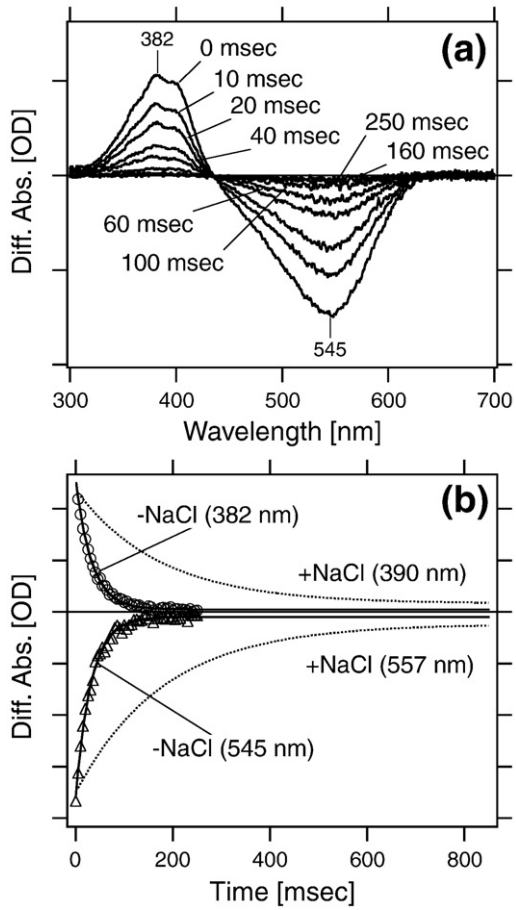

Fig. 6. (a) Flash-induced difference spectra of DDM-solubilized *Sr*SRI in the absence of NaCl over a spectral range from 300 to 700 nm and a time range from 5 to 250 ms. Samples were resuspended in 50 mM Tris–H_2SO_4, pH 7.0, and 0.1% DDM with 333 mM Na_2SO_4. The curves are spectra of 0, 10, 20, 40, 60, 100, 160, and 250 ms after the illumination. The temperature was kept at 25 °C. (b) Flash-induced kinetic data of *Sr*SRI in the absence of NaCl at 382 nm representing the M decay and 545 nm representing the recovery of the initial state. The kinetic data of *Sr*SRI with 1 M NaCl (dotted line) were reproduced from a previous study to compare the time range with that in the absence of NaCl. For *Sr*SRI with 1 M NaCl, the M intermediate and the initial state were monitored at 390 and 557 nm, respectively. One division of the *y*-axis of (a) and (b) corresponds to 0.05 and 0.02 absorbance units, respectively.

activation of its transducer protein, HtrI.[13] We analyzed the decay of the M intermediate using time-resolved laser spectroscopy. Figure 6a shows the light minus dark difference spectra of *Sr*SRI without NaCl (333 mM Na_2SO_4) over the spectral range at 300 to 700 nm. The spectra have an isosbestic point at about 430 nm, indicating the linear reaction from M to the original state. Depletion by flash and recovery of the orange pigment were observed at 545 nm, a λ_{max} almost the same as the absorption maximum of *Sr*SRI in desalted conditions (as shown in Fig. 2a). The λ_{max} of *Sr*SRI without NaCl (333 mM Na_2SO_4) is red-shifted 8 nm, from 382 to 390 nm. At 382 nm, increased or decreased absorbances were observed, implying the formation and decay of the M intermediate. Figure 6b shows the time courses of the absorbance change at 382 nm for the M state and at 545 nm for the original state without NaCl (333 mM Na_2SO_4). The absorbance changes at 382 nm fit well to a single exponential decay equation, and the decay half-time was estimated as 25 ms. The kinetic data of *Sr*SRI with 1 M NaCl were reproduced from a previous study for comparison where curves at 390 and 557 nm are for the M state and the original state, respectively.[25] The decay half-time has been estimated as 320 ms. It should be noted that 1 M NaCl is enough for *Sr*SRI to bind the chloride ion because the K_m value is about 300 mM (Fig. 3). Thus, the photocycle of *Sr*SRI without NaCl (333 mM Na_2SO_4) became 13 times faster than that with 1 M NaCl. These chloride ion dependencies of *Sr*SRI and a schematic of the photocycle of *Sr*SRI in the presence or absence of NaCl are shown in Table 1 and in Fig. 9b, respectively, with those of other retinal proteins, BR, *Np*HR, *Np*SRII, and *Hs*SRI.[22,30–35] Using low-temperature UV–Vis spectroscopy, the two-photon reaction product, P525, the intermediate important for negative phototaxis, was observed in *Sr*SRI without salt as well as in *Sr*SRI with NaCl, whose λ_{max} is about 520 nm (data not shown).[25]

Table 1. Effects of chloride ions on the photochemical properties of microbial rhodopsins

	Cl^-	λ_{max} (nm)	$\Delta\upsilon$ (cm^{-1})	K_m for Cl^- (mM)
*Sr*SRI	+	556*[25]	−130	300
	−	542		
*Hs*SRI	+	587*[30]	?	?
	−	ND		
*Np*SRII	+	498*[31]	0	~400*[22]
	−	498*[32]		
BR	+	569*[33]	0	ND
	−	569*[33]		
*Np*HR	+	577*[34]	664	5*[35]
	−	600*[34]		

Site-directed mutagenesis studies on the Cl^--binding site

To identify the residue(s) involved in the chloride binding, we constructed *Sr*SRI mutants containing the replacement of conserved basic amino acid residues among SRI family (R69A, R92A, R210A, H131A, and H131F, see Fig. 1). UV–Vis absorption spectra of purified *Sr*SRI mutants over the spectral

Fig. 7. Effect of chloride ion binding on the absorption spectrum of DDM-solubilized *Sr*SRI for (a) WT, (b) R69A, (c) R92A, (d) R210A, (e) H131A, and (f) H131F with 1 M NaCl (dotted line) and 333 mM Na_2SO_4 (continuous line). The samples were suspended in 50 mM Tris–H_2SO_4, pH 7.0, and 0.1% DDM. (a) was reproduced from Fig. 2. One division of *y*-axis corresponds to 0.2 absorbance units.

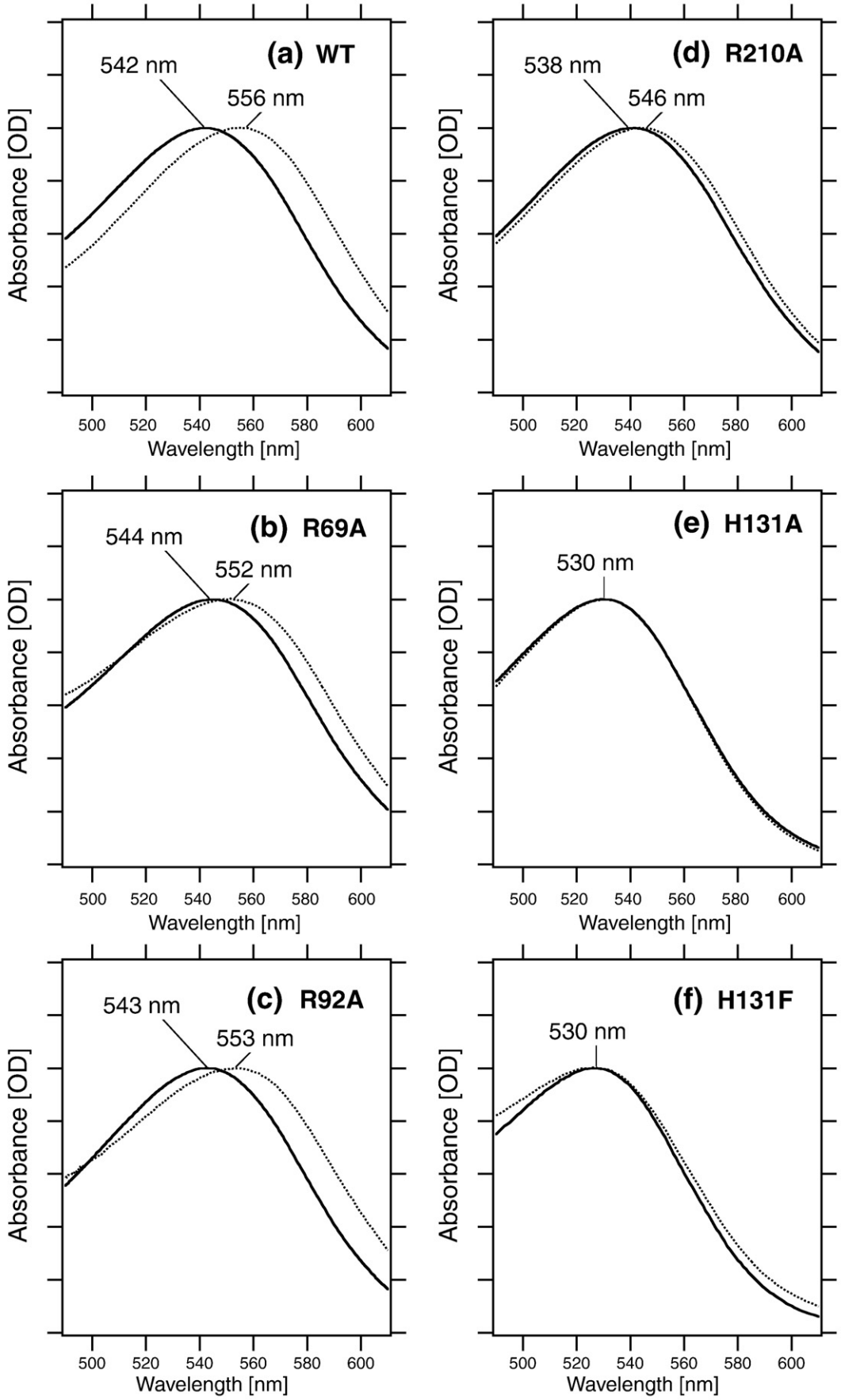

Fig. 7 (*legend on previous page*)

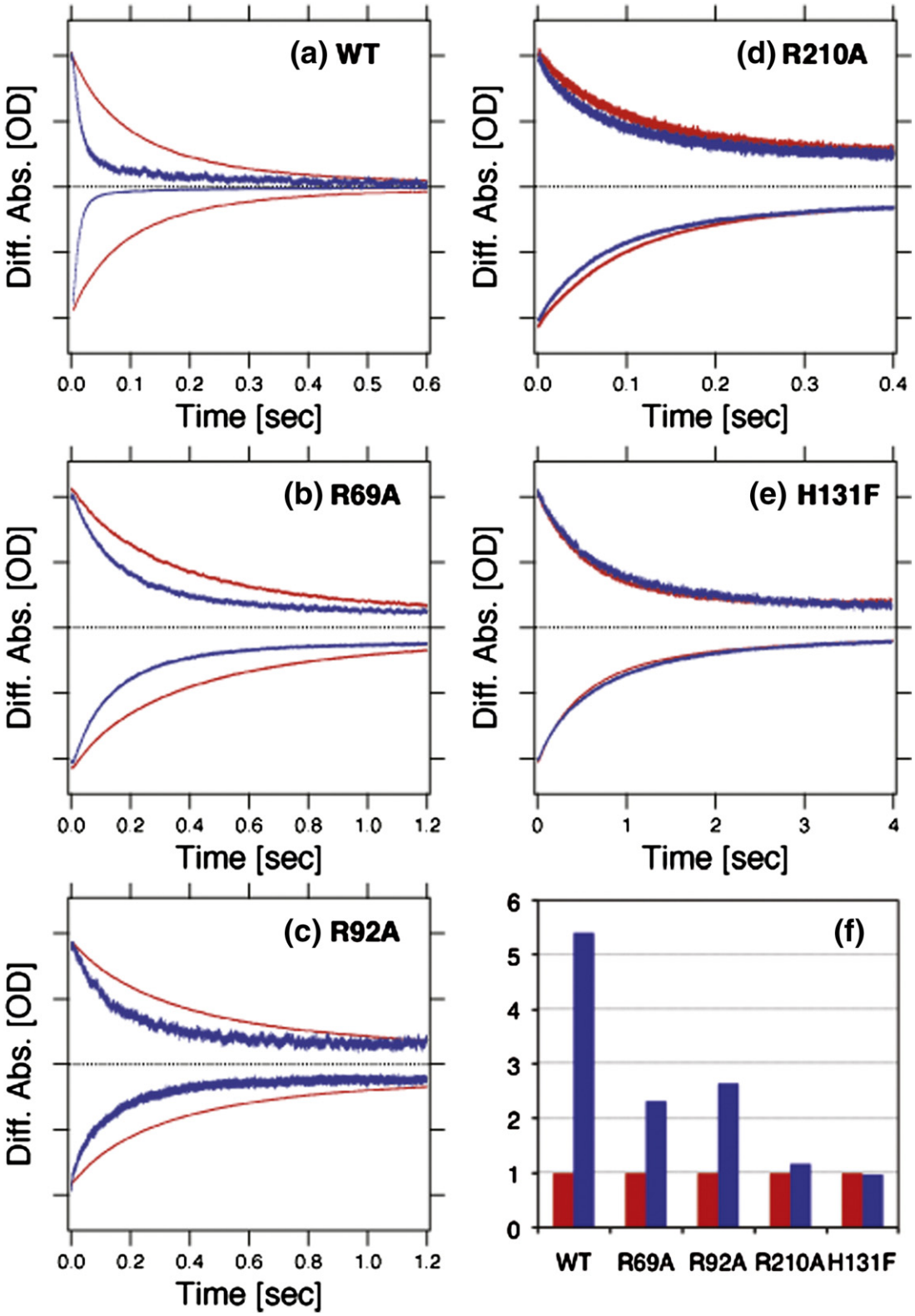

Fig. 8. Strobe-flash-induced kinetic data of *Sr*SRI for (a) WT, (b) R69A, (c) R92A, (d) R210A, and (e) H131F with 1 M NaCl (red curves) and 333 mM Na_2SO_4 (blue curves). The samples were suspended in 50 mM Tris–H_2SO_4, pH 7.0, and 0.1% DDM. The temperature was kept at 25 °C. One division of *y*-axis corresponds to 10 mOD. The M intermediate and initial state of *Sr*SRI were monitored at 390 and 550 nm, respectively. (f) Relative time constants of M decay in buffer containing 333 mM Na_2SO_4 (blue) or 1 M NaCl (red).

range from 490 to 610 nm were obtained as shown in Fig. 7. R69A (Fig. 7b), R92A (Fig. 7c), and R210A (Fig. 7d) mutants showed 8 nm (−266 cm^{-1}), 10 nm (−333 cm^{-1}), and 8 nm (−272 cm^{-1}) spectral red shift with the chloride-dependent manner (continuous line, 333 mM Na_2SO_4; dotted line, 1 M NaCl), respectively, whereas H131A (Fig. 7e) and H131F (Fig. 7f) mutants did not alter the absorption maximum, and the λ_{max} of the mutants (530 nm) was similar to that of Cl^--free *Sr*SRI (542 nm), indicating that His131 of *Sr*SRI participates in the Cl^--binding site. The shift from 542 to 530 nm may suggest that His131 is also involved in color tuning. His131 mutants with and without NaCl contain more than 88% *all-trans* retinal with a small proportion of *13-cis* retinal as well as wild-type *Sr*SRI, indicating that the spectral blue shift is not caused by a change in retinal configuration.

We also investigated whether the photocycle of these mutants is affected by the chloride ion. In the flash-photolysis experiments, His131 mutants lost the activity by laser accumulation. Therefore, strobe flash spectroscopy is employed here instead of laser. Figure 8 shows the decay of the M intermediate and the recovery of the original state. The photocycle kinetics of WT (Fig. 8a) is identical with that in Fig. 6b. R69A (Fig. 8b), R92A (Fig. 8c), and R210A (Fig. 8d) without NaCl (333 mM Na_2SO_4) become faster than that with 1 M NaCl, whereas H131F mutant did not alter the photocycle kinetics. The relative time constant with and without NaCl is shown in Fig. 8f. We were not able to measure the kinetics of the H131A mutant because of the instability. Thus, these results strongly suggest that the H131 residue is involved in chloride-binding site.

Discussion

Importance of chloride ion binding for the function of *Sr*SRI

The archaea *H. salinarum* and *N. pharaonis* are found in highly halophilic environments, such as saltern crystallizer ponds.[19,36] The eubacterium *S. ruber* is also an extremely halophilic bacterium, which requires at least 200 g NaCl per liter (>3 M) to survive.[19] Thus, archaeal rhodopsins (BR, HR, SRI, and SRII) and *Sr*SRI function in the presence of high concentrations of NaCl in the environment where the microbes live, suggesting the possible effect(s) of salts on the function of their retinal proteins. In fact, the effects of Cl^- binding to microbial rhodopsins on their photochemical and functional properties have been reported previously[22,34] and are listed in Table 1. In the SRI family, the effects of chloride are unclear because of the instability of *Hs*SRI protein in the absence of salt. In this study, we used *Sr*SRI, which has a relatively high stability even in the absence of salts.[25]

It is well known that the ion-pumping rhodopsins have been optimized by nature to have relatively fast photocycling rates, making them efficient pumps, whereas the sensory receptors, including *Sr*SRI, have slow photocycles to activate a phosphorylation cascade controlling flagellar motor rotation.[13,27] In *Sr*SRI, M390 is believed to be an active intermediate having a slow decay (Fig. 9b).[25] As shown in Fig. 6, the photocycling rate of *Sr*SRI without NaCl (τ = 25 ms) became 13 times faster than that in the presence of 1 M NaCl (τ = 320 ms), which is relatively close to that of an ion-pumping rhodopsin, BR (τ = 5 ms). For the K intermediate, the molar extinction coefficient is affected by the chloride ion binding, indicating that the chloride ion binds not only to the original state ($SrSRI_{542}$) but also to the K and M intermediates, and is important for the slow photocycle. Thus, it is likely that chloride ion binding to *Sr*SRI is important for its function in phototaxis.

Chloride-binding site in *Sr*SRI

An interesting question arises as to where is the chloride-binding site in *Sr*SRI, although all microbial rhodopsins are highly similar in their primary and tertiary structures,[8,16–18] especially in the chromophore binding site? Microbial rhodopsins are covalently bound to an *all-trans* retinal chromophore at a conserved lysine residue on the G-helix via a PSB bond.[27] The PSB of all-trans retinal shows λ_{max} at approximately 440 nm in methanol.[37] On the other hand, when *all-trans* retinal binds to an apoprotein (called an opsin) to form a PSB, a large spectral red shift ('opsin shift') is observed.[38] The term 'opsin shift' is also used to refer to the difference in λ_{max} among pigments. The absorption maximum of a chromophore corresponds to its lowest $\pi - \pi*$ excitation energy. In the ground state, a positive charge is localized mainly on the Schiff base nitrogen, and upon excitation, it shifts toward the β-ionone ring. Accordingly, various factors can lead to changes in the energy gap between the ground and excited states. Empirical and theoretical studies have suggested several mechanisms by which the opsin shift occurs.[39] They include the following:[40–44] (i) the strength of the electrostatic interaction between the PSB and its counterion or hydrogen bond acceptor, (ii) an alteration in the polarity or polarizability of the chromophore-binding site environment caused by the arrangement of polar or aromatic residues, and (iii) an isomerization around the 6-S bond, which connects the polyene chain to the β-ionone ring.

Among the microbial rhodopsins, SRII and HR can bind to chloride ion(s) unlike BR (Fig. 1) at neutral pH. It should be noted that BR binds chloride, although only at pH below 1.[45] The X-ray crystal structure and photochemical analysis of *Np*SRII reveal that Arg72 and Asp193, which are located near the extracellular side, are important for chloride ion binding.[23,24,46] The binding affinity is estimated to ~400 mM,[22] which is close to that of *Sr*SRI (307 mM); however, the Asp193 of *Np*SRII is not conserved in SRIs and the chloride binding to *Np*SRII does not alter the absorption maximum.[31]

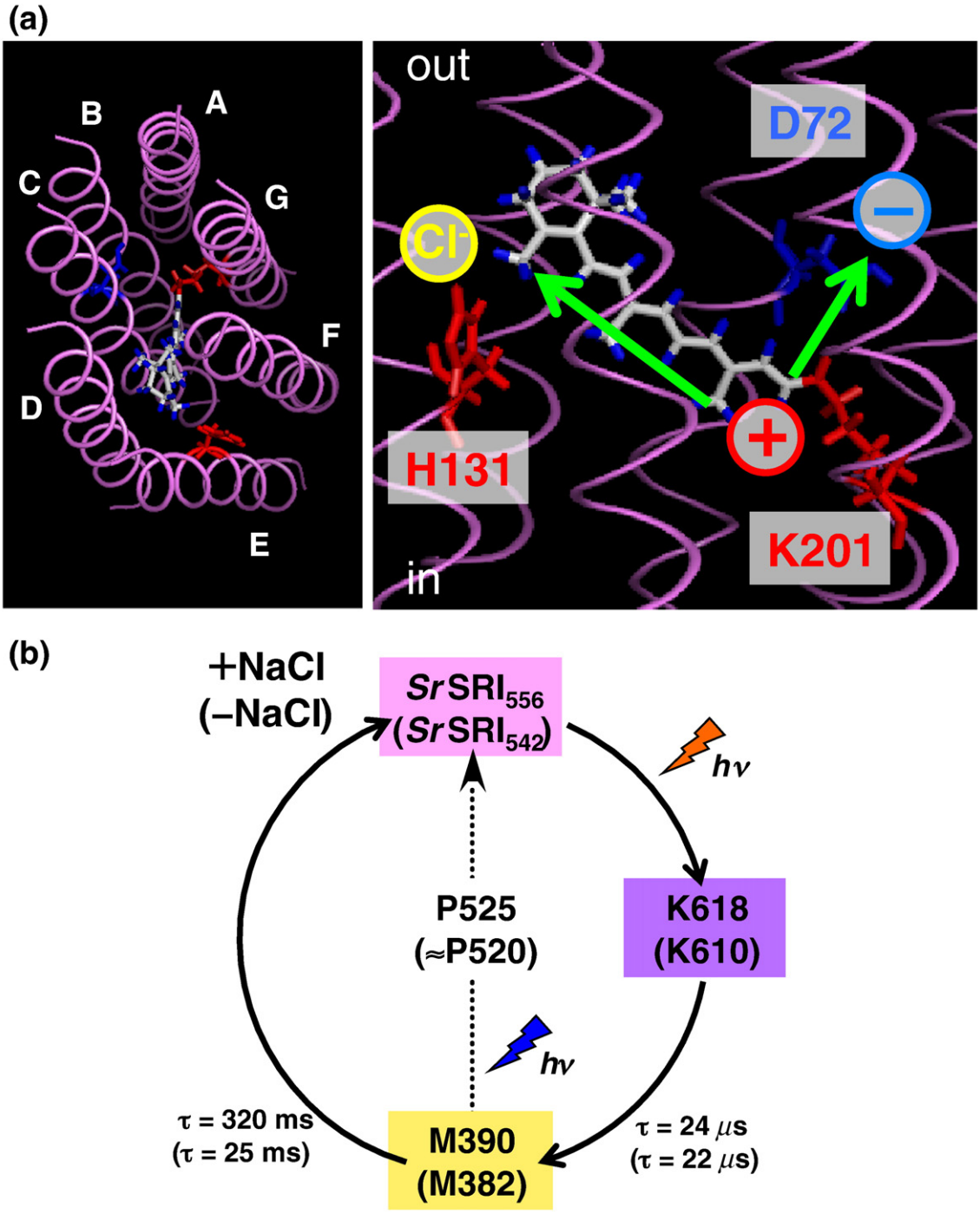

Fig. 9. (a) Putative chloride-binding site of *Sr*SRI (left, top view; right, side view). The structure was generated using theoretical model of *Hs*SRI (Protein Data Bank ID: 1SR1).[50] It was assumed that a positive charge locating on the Schiff base nitrogen is likely to move to the β-ionone ring by chloride ion binding to His131. (b) Scheme of the photochemical reaction cycle of *Sr*SRI with or without 1 M NaCl. *hυ* indicates light-dependent reactions, and the other arrows represent thermal reactions. Light absorption of *Sr*SRI triggers cyclic chemical reactions consisting of some sequential intermediate states.[25] The decay rates of the K and the M intermediates are obtained by a single exponential equation by the flash-photolysis experiments shown in Figs. 5 and 6 and in a previous study.[25] The estimated absorption maxima of the original state and the K and the M intermediates are shown in this figure, where those of the K and the M intermediates with NaCl are consistent with a previous study.[25]

Thus, it is likely that a corresponding binding site in *Sr*SRI exists in other position near the retinal molecule because its λ_{max} is affected by the chloride ion binding. HR shows a spectral blue shift by titration with NaCl.[34] The spectrum of *Np*HR without Cl^- (λ_{max} = 600 nm) is shifted to a shorter wavelength by the addition of 1 M NaCl (λ_{max} = 577 nm).[20] However, the chloride ion binds near the PSB (Fig. 1),

and the λ_{max} shifts to a shorter wavelength [$\Delta = -23$ nm ($\Delta\upsilon = 664$ cm^{-1})]. In contrast, the λ_{max} of *Sr*SRI shifts to a longer wavelength [$\Delta = +14$ nm ($\Delta\upsilon = -130$ cm^{-1})], which is the opposite direction compared with *Np*HR. In addition, the chloride binding to *Sr*SRI does not alter the pK_a of the counterion (Fig. 2), indicating that the binding site is located near the polyene chain and/or the β-ionone ring. In the case of red pigments in animals, the chloride ion binds to His and Lys residues located at the extracellular loop,[47] and the binding alters the charge distribution of the PSB. The λ_{max} shifts to a longer wavelength ($\Delta = +40$ nm), which is the same direction compared with *Sr*SRI; however, those residues are not conserved in *Sr*SRI, and retinal chromophores of red pigment and *Sr*SRI are located at different positions, near the surface for red pigments and in the middle of the transmembrane region for *Sr*SRI, indicating that a corresponding binding site does not exist in *Sr*SRI.

In retinal proteins, the binding sites are constructed by charged residues (Asp, Glu, Lys, Arg and His), and therefore, they are good candidates for chloride-binding sites. Figures 7 and 8 strongly suggest that the conserved residue, His131 of *Sr*SRI, is involved in the Cl^--binding site, and this is a novel binding site among rhodopsins. It is assumed that a positive charge locating on the Schiff base nitrogen moves to the β-ionone ring by chloride ion binding to His131 (Fig. 9a). The changes of charge distribution cause the changes discussed in possibilities (i), (ii), and/or (iii) above. Although the high-resolution structure of SRI is not solved, it is predicted that the space around His131 is significantly narrow for the Cl^- binding, suggesting the large structural changes of *Sr*SRI upon Cl^- binding. Interestingly, we found that SRI from the archaeon *Haloarcula vallismortis* (*Hv*SRI) exhibited similar alterations due to chloride ion binding (unpublished data). The binding to *Sr*SRI is likely to be important for the function of the SRI protein family.

Materials and Methods

Preparation of *Sr*SRI samples

*Sr*SRI was prepared as described previously.[25] Briefly, *Sr*SRI proteins with a six-histidine tag at the C-terminus were expressed in *Escherichia coli* BL21 (DE3) cells as a recombinant protein, solubilized with 1.0% DDM, and purified with a Ni^{2+}-NTA column (QIAGEN, Valencia, CA, USA) and an ion-exchange column (HiTrapQ, GE Healthcare, UK).[25] The purified sample was reconstituted into PG liposomes (*Sr*SRI:PG = 1:50 molar ratio) by removing the detergent with Bio-Beads (SM-2, Bio-Rad, Hercules, CA, USA).[26] The *Sr*SRI mutant genes R69A, R92A, R210A, H131A, and H131F were constructed by PCR using the QuikChange Site-Directed Mutagenesis Kit (Stratagene, La Jolla, CA, USA) as described previously.[48]

UV–Vis spectroscopy

For the binding assay, each purified *Sr*SRI sample in DDM detergent micelles was resuspended in buffer (50 mM Tris–H_2SO_4, pH 7.0, and 0.1% DDM) and was passed through an Amicon Ultra ultrafiltration filter (Molecular cutoff, 10,000; Millipore, Bedford, MA, USA). NaCl or various salts (NaI, NaBr, NaF, $NaNO_3$, or Na_2SO_4) were then added to the sample. Spectra were obtained by using a UV2450 spectrophotometer (Shimadzu, Kyoto, Japan). For pH titration of the counterion Asp72, the spectra were obtained by using the UV2450 spectrophotometer with an ISR-2200 integrating sphere (Shimadzu). Each PG-reconstituted sample was resuspended in the buffer solution mixed with six types of buffers having different pK_a {citric acid, Mes (4-morpholineethanesulfonic acid), Hepes, Mops, Ches, or Caps [3-(cyclohexylamino)propane-1-sulfonic acid], 10 mM each}[49] with 333 mM Na_2SO_4. The pH was then adjusted to the desired value by the addition of concentrated H_2SO_4.

High-performance liquid chromatography

HPLC analysis was performed as described previously.[25] Samples were analyzed in buffer (50 mM Tris–H_2SO_4, pH 7.0, with 0.1% DDM) containing 1 M NaCl or no NaCl where the ionic strength was kept constant by 333 mM Na_2SO_4. Extraction of retinal oxime from the sample was carried out with hexane after denaturation by methanol and 500 mM hydroxylamine at 4 °C. The molar compositions of retinal isomers were calculated from the areas of the peaks monitored at 360 nm.

Time-resolved laser spectroscopy

For measurements of the K intermediate, the purified samples were resuspended in buffer (50 mM Tris–H_2SO_4, pH 7.0, and 0.1% DDM) with 1 M NaCl or without NaCl, where the ionic strength was kept constant by 333 mM Na_2SO_4. The second harmonic light from a Nd–YAG laser ($\lambda = 532$ nm, Minilite II Continuum, Santa Clara, CA, USA) with a pulse width of ~6 ns was used for excitation of the sample solutions. The energy of the pump laser was 50 μJ/pulse. For recording absorption changes over a range from 433 to 696 nm at various times after excitation, light from a Xe lamp (Hamamatsu Photonics, Hamamatsu, Japan) was introduced to the sample by a counter-propagation geometry to the excitation light. The probe light was led to a monochrometer (SpectraPro 2300i, Princeton Instruments/Acton, Trenton, NJ, USA) by an optical fiber and was detected using an ICCD camera system (PI-MAX/PI-MAX2 System, Princeton Instruments). Transient absorption spectra were measured at various time points from $t = 1$ μs to 1 ms using this setup. Sample solutions were placed in quartz cells and the absorbance was adjusted to ~0.7 at the excitation wavelength (532 nm). The temperature of each sample was kept at 25 °C.

For measurements of the M intermediate, the apparatus and the procedure for analysis were essentially the same as described previously.[25] Each purified sample was resuspended in buffer (50 mM Tris–H_2SO_4, pH 7.0, and 0.1% DDM) with 333 mM Na_2SO_4. Flash-induced absorption changes were acquired with a 5-ms interval by using a commercial flash-photolysis system (Hamamatsu Photonics) as described previously.[25] Excitation of each *Sr*SRI sample was done using 545-nm nanosecond laser pulses from a Nd–YAG laser apparatus (LS-2134UT-10; LOTIS TII: 355 nm, 7 ns, 60 mJ) through an Optical Parametric Oscillator (LT-2214-OPO/PM; LOTIS TII). The energy of one laser pulse was 3.3 mJ. For signal-to-noise improvement, 40 photoreactions were averaged for one time slice, and two sets of time-resolved light-induced difference spectra were recorded and averaged for each sample solution. Absorbance at the λ_{max} (547 nm) was 0.60 and 0.48 before and after the experiment, respectively (the laser-induced bleach of the sample was 20%), while the kinetics of the two experiments were almost identical. The temperature of each sample was kept at 25 °C.

Time-resolved strobe flash spectroscopy

A conventional flash-photolysis apparatus was constructed for the measurements in the long time range. The actinic flashes (>520 nm; duration, 200 ms) were obtained by a Xenon flash lamp (PE-60SG, Panasonic Photo & Lighting Co., Ltd., Japan) in combination with a yellow glass filter (Y-52, AGC, Japan) and a neutral density filter (AND-50S-25, SIGMA KOKI, Japan). The source of monitoring light was a 150-W halogen lamp (JASCO, Japan), and the beam was perpendicular to that of the actinic flash. The photosensor module (H8249-102, Hamamatsu Photonics) was used to detect the light passing through the sample. To select the measuring wavelength and exclude the scattered actinic flash from the sample, we placed two monochromators (CT-10, JASCO, Japan) in the rear of the monitoring light source and in front of the photosensor module. The output of the photosensor module was further amplified and filtered by a homemade amplifier and then stored in a computer. Though a phototransient signal could be acquired with a single flash, several kinetic traces were averaged to improve the signal-to-noise ratio.

Acknowledgements

We thank Dr. Akira Kawanabe for assistance with the HPLC analysis and Dr. Tomomi Kitajima-Ihara and Ms. Akiko Okada for their encouragement. The present work was financially supported in part by a Grant-in-Aid for Scientific Research (KAKENHI) on Priority Area (Area No. 477) from the Ministry of Education, Culture, Sports, Science and Technology of Japan. This work was also supported by grants from the Japanese Ministry of Education, Culture, Sports, Science, and Technology to Y.F, (19042013 and 19045015), to H.K. (19370067 and 20050015), and to Y.S. (20050012).

References

1. Kandori, H., Shichida, Y. & Yoshizawa, T. (2001). Photoisomerization in rhodopsin. *Biochemistry (Moscow)*, **66**, 1197–1209.
2. Wada, M. & Suetsugu, N. (2004). Plant organelle positioning. *Curr. Opin. Plant Biol.* **7**, 626–631.
3. Spudich, J. L. (2006). The multitalented microbial sensory rhodopsins. *Trends Microbiol.* **14**, 480–487.
4. Oesterhelt, D. & Stoeckenius, W. (1971). Rhodopsin-like protein from the purple membrane of *Halobacterium halobium*. *Nat. New Biol.* **233**, 149–152.
5. Essen, L. O. (2002). Halorhodopsin: light-driven ion pumping made simple? *Curr. Opin. Struct. Biol.* **12**, 516–522.
6. Bogomolni, R. A. & Spudich, J. L. (1982). Identification of a third rhodopsin-like pigment in phototactic *Halobacterium halobium*. *Proc. Natl Acad. Sci. USA*, **79**, 6250–6254.
7. Wolff, E. K., Bogomolni, R. A., Scherrer, P., Hess, B. & Stoeckenius, W. (1986). Color discrimination in halobacteria: spectroscopic characterization of a second sensory receptor covering the blue-green region of the spectrum. *Proc. Natl Acad. Sci. USA*, **83**, 7272–7276.
8. Lanyi, J. K. (2004). Bacteriorhodopsin. *Annu. Rev. Physiol.* **66**, 665–688.
9. Chen, X. & Spudich, J. L. (2002). Demonstration of 2:2 stoichiometry in the functional SRI–HtrI signaling complex in *Halobacterium* membranes by gene fusion analysis. *Biochemistry*, **41**, 3891–3896.
10. Gordeliy, V. I., Labahn, J., Moukhametzianov, R., Efremov, R., Granzin, J., Schlesinger, R. *et al.* (2002). Molecular basis of transmembrane signalling by sensory rhodopsin II–transducer complex. *Nature*, **419**, 484–487.
11. Takahashi, T., Mochizuki, Y., Kamo, N. & Kobatake, Y. (1985). Evidence that the long-lifetime photointermediate of *s*-rhodopsin is a receptor for negative phototaxis in *Halobacterium halobium*. *Biochem. Biophys. Res. Commun.* **127**, 99–105.
12. Spudich, J. L. & Bogomolni, R. A. (1984). Mechanism of colour discrimination by a bacterial sensory rhodopsin. *Nature*, **312**, 509–513.
13. Hoff, W. D., Jung, K. H. & Spudich, J. L. (1997). Molecular mechanism of photosignaling by archaeal sensory rhodopsins. *Annu. Rev. Biophys. Biomol. Struct.* **26**, 223–258.
14. Rudolph, J., Tolliday, N., Schmitt, C., Schuster, S. C. & Oesterhelt, D. (1995). Phosphorylation in halobacterial signal transduction. *EMBO J.* **14**, 4249–4257.
15. Luecke, H., Schobert, B., Richter, H. T., Cartailler, J. P. & Lanyi, J. K. (1999). Structure of bacteriorhodopsin at 1.55 Å resolution. *J. Mol. Biol.* **291**, 899–911.
16. Kolbe, M., Besir, H., Essen, L. O. & Oesterhelt, D. (2000). Structure of the light-driven chloride pump halorhodopsin at 1.8 Å resolution. *Science*, **288**, 1390–1396.
17. Luecke, H., Schobert, B., Lanyi, J. K., Spudich, E. N. & Spudich, J. L. (2001). Crystal structure of sensory rhodopsin II at 2.4 Å: insights into color tuning and transducer interaction. *Science*, **293**, 1499–1503.
18. Royant, A., Nollert, P., Edman, K., Neutze, R., Landau,

E. M., Pebay-Peyroula, E. & Navarro, J. (2001). X-ray structure of sensory rhodopsin II at 2.1 Å resolution. *Proc. Natl Acad. Sci. USA*, **98**, 10131–10136.
19. Anton, J., Rossello-Mora, R., Rodriguez-Valera, F. & Amann, R. (2000). Extremely halophilic bacteria in crystallizer ponds from solar salterns. *Appl. Environ. Microbiol.* **66**, 3052–3057.
20. Sato, M., Kubo, M., Aizawa, T., Kamo, N., Kikukawa, T., Nitta, K. & Demura, M. (2005). Role of putative anion-binding sites in cytoplasmic and extracellular channels of *Natronomonas pharaonis* halorhodopsin. *Biochemistry*, **44**, 4775–4784.
21. Rudiger, M. & Oesterhelt, D. (1997). Specific arginine and threonine residues control anion binding and transport in the light-driven chloride pump halorhodopsin. *EMBO J.* **16**, 3813–3821.
22. Iwamoto, M., Hasegawa, C., Sudo, Y., Shimono, K., Araiso, T. & Kamo, N. (2004). Proton release and uptake of *pharaonis* phoborhodopsin (sensory rhodopsin II) reconstituted into phospholipids. *Biochemistry*, **43**, 3195–3203.
23. Iwamoto, M., Furutani, Y., Sudo, Y., Shimono, K., Kandori, H. & Kamo, N. (2002). Role of Asp193 in chromophore–protein interaction of *pharaonis* phoborhodopsin (sensory rhodopsin II). *Biophys. J.* **83**, 1130–1135.
24. Kitade, Y., Furutani, Y., Kamo, N. & Kandori, H. (2009). Proton release group of *pharaonis* phoborhodopsin revealed by ATR–FTIR spectroscopy. *Biochemistry*, **48**, 1595–1603.
25. Kitajima-Ihara, T., Furutani, Y., Suzuki, D., Ihara, K., Kandori, H., Homma, M. & Sudo, Y. (2008). *Salinibacter* sensory rhodopsin: sensory rhodopsin I-like protein from a eubacterium. *J. Biol. Chem.* **283**, 23533–23541.
26. Suzuki, D., Sudo, Y., Furutani, Y., Takahashi, H., Homma, M. & Kandori, H. (2008). Structural changes of *Salinibacter* sensory rhodopsin I upon formation of the K and M photointermediates. *Biochemistry*, **47**, 12750–12759.
27. Haupts, U., Tittor, J. & Oesterhelt, D. (1999). Closing in on bacteriorhodopsin: progress in understanding the molecule. *Annu. Rev. Biophys. Biomol. Struct.* **28**, 367–399.
28. Sudo, Y., Iwamoto, M., Shimono, K. & Kamo, N. (2002). Tyr-199 and charged residues of *pharaonis* phoborhodopsin are important for the interaction with its transducer. *Biophys. J.* **83**, 427–432.
29. Zhang, Y. & Cremer, P. S. (2006). Interactions between macromolecules and ions: the Hofmeister series. *Curr. Opin. Chem. Biol.* **10**, 658–663.
30. Spudich, J. L., Zacks, D. N. & Bogomolni, R. A. (1995). Microbial sensory rhodopsins: photochemistry and function. *Israel J. Chem.* **35**, 495–513.
31. Shimono, K., Kitami, M., Iwamoto, M. & Kamo, N. (2000). Involvement of two groups in reversal of the bathochromic shift of *pharaonis* phoborhodopsin by chloride at low pH. *Biophys. Chem.* **87**, 225–230.
32. Miyazaki, M., Hirayama, J., Hayakawa, M. & Kamo, N. (1992). Flash photolysis study on *pharaonis* phoborhodopsin from a haloalkaliphilic bacterium (*Natronobacterium pharaonis*). *Biochim. Biophys. Acta*, **1140**, 22–29.
33. Lanyi, J. K. (1998). Understanding structure and function in the light-driven proton pump bacteriorhodopsin. *J. Struct. Biol.* **124**, 164–178.
34. Scharf, B. & Engelhard, M. (1994). Blue halorhodopsin from *Natronobacterium pharaonis*: wavelength regulation by anions. *Biochemistry*, **33**, 6387–6393.
35. Sato, M., Kikukawa, T., Araiso, T., Okita, H., Shimono, K., Kamo, N. *et al.* (2003). Roles of Ser130 and Thr126 in chloride binding and photocycle of *pharaonis* halorhodopsin. *J. Biochem.* **134**, 151–158.
36. Oesterhelt, D. & Stoeckenius, W. (1973). Functions of a new photoreceptor membrane. *Proc. Natl Acad. Sci. USA*, **70**, 2853–2857.
37. Pitt, G. A., Collins, F. D., Morton, R. A. & Stok, P. (1955). Studies on rhodopsin. VIII. Retinylidenemethylamine, an indicator yellow analogue. *Biochem. J.* **59**, 122–128.
38. Nakanishi, K., Balogh-Nair, V., Arnaboldi, M., Tsujimoto, K. & Honig, B. (1980). An external point-charge model for bacteriorhodopsin to account for its purple color. *J. Am. Chem. Soc.* **102**, 7945–7947.
39. Shimono, K., Ikeura, Y., Sudo, Y., Iwamoto, M. & Kamo, N. (2001). Environment around the chromophore in *pharaonis* phoborhodopsin: mutation analysis of the retinal binding site. *Biochim. Biophys. Acta*, **1515**, 92–100.
40. Blatz, P. E., Mohler, J. H. & Navangul, H. V. (1972). Anion-induced wavelength regulation of absorption maxima of Schiff bases of retinal. *Biochemistry*, **11**, 848–855.
41. Honig, B., Dinur, U., Nakanishi, K., Balogh-Nair, V., Gawinowicz, M. A., Arnaboldi, M. & Motto, M. G. (1979). An external point-charge model for wavelength regulation in visual pigments. *J. Am. Chem. Soc.* **101**, 7084–7086.
42. Hu, J., Griffin, R. G. & Herzfeld, J. (1994). Synergy in the spectral tuning of retinal pigments: complete accounting of the opsin shift in bacteriorhodopsin. *Proc. Natl Acad. Sci. USA*, **91**, 8880–8884.
43. Rajamani, R. & Gao, J. (2002). Combined QM/MM study of the opsin shift in bacteriorhodopsin. *J. Comput. Chem.* **23**, 96–105.
44. Yan, B., Spudich, J. L., Mazur, P., Vunnam, S., Derguini, F. & Nakanishi, K. (1995). Spectral tuning in bacteriorhodopsin in the absence of counterion and coplanarization effects. *J. Biol. Chem.* **270**, 29668–29670.
45. Kelemen, L., Galajda, P., Szaraz, S. & Ormos, P. (1999). Chloride ion binding to bacteriorhodopsin at low pH: an infrared spectroscopic study. *Biophys. J.* **76**, 1951–1958.
46. Ikeura, Y., Shimono, K., Iwamoto, M., Sudo, Y. & Kamo, N. (2004). Role of Arg-72 of pharaonis Phoborhodopsin (sensory rhodopsin II) on its photochemistry. *Biophys. J.* **86**, 3112–3120.
47. Wang, Z., Asenjo, A. B. & Oprian, D. D. (1993). Identification of the Cl(−)-binding site in the human red and green color vision pigments. *Biochemistry*, **32**, 2125–2130.
48. Sudo, Y., Furutani, Y., Shimono, K., Kamo, N. & Kandori, H. (2003). Hydrogen bonding alteration of Thr-204 in the complex between *pharaonis* phoborhodopsin and its transducer protein. *Biochemistry*, **42**, 14166–14172.
49. Chizhov, I., Schmies, G., Seidel, R., Sydor, J. R., Luttenberg, B. & Engelhard, M. (1998). The photophobic receptor from *Natronobacterium pharaonis*: temperature and pH dependencies of the photocycle of sensory rhodopsin II. *Biophys. J.* **75**, 999–1009.
50. Lin, S. L. & Yan, B. (1997). Three-dimensional model of sensory rhodopsin I reveals important restraints between the protein and the chromophore. *Protein Eng.* **10**, 197–206.